Co-transplantation of tonsil-derived mesenchymal stromal cells in bone marrow transplantation promotes thymus regeneration and T cell diversity following cytotoxic conditioning

DA-WON CHOI[1], KYUNG-AH CHO[1], HYUN-JI LEE[1], YU-HEE KIM[1], KYONG-JE WOO[2],
JOO-WON PARK[3], KYUNG-HA RYU[4] and SO-YOUN WOO[1]

Departments of [1]Microbiology, [2]Plastic and Reconstructive Surgery, [3]Biochemistry and [4]Pediatrics,
College of Medicine, Ewha Womans University, Seoul 07804, Republic of Korea

Abstract. Bone marrow (BM) transplantation (BMT) represents a curative treatment for various hematological disorders. Prior to BMT, a large amount of the relevant anticancer drug needed to be administered to eliminate cancer cells. However, during this pre-BMT cytotoxic conditioning regimen, hematopoietic stem cells in the BM and thymic epithelial cells were also destroyed. The T cell receptor (TCR) recognizes diverse pathogen, tumor and environmental antigens, and confers immunological memory and self-tolerance. Delayed thymus reconstitution following pre-BMT cytotoxic conditioning impedes *de novo* thymopoiesis and limits T cell-mediated immunity. Several cytokines, such as RANK ligand, interleukin (IL)-7, IL-22 and stem cell factor, were recently reported to improve thymopoiesis and immune function following BMT. In the present study, it was found that the co-transplantation of tonsil-derived mesenchymal stromal cells (T-MSCs) with BM-derived cells (BMCs) accelerated the recovery of involuted thymuses in mice following partial pre-BMT conditioning with busulfan-cyclophosphamide treatment, possibly by inducing FMS-like tyrosine kinase 3 ligand (FLT3L) and fibroblast growth factor 7 (FGF7) production in T-MSCs. The co-transplantation of T-MSCs with BMCs also replenished the CD3+ cell population by inhibiting thymocyte apoptosis following pre-BMT cytotoxic conditioning. Furthermore, T-MSC co-transplantation improved the recovery of the TCR repertoire and led to increased thymus-generated T cell diversity.

Correspondence to: Professor So-Youn Woo, Department of Microbiology, College of Medicine, Ewha Womans University, 25 Magokdong-ro 2-gil, Gangseo-gu, Seoul 07804, Republic of Korea
E-mail: soyounwoo@ewha.ac.kr

Introduction

Allogenic bone marrow (BM) transplantation (BMT) is the standard treatment for a number of hematopoietic disorders, such as aplastic anemia and leukemia. However, several challenges related to allogenic BMT exist, including cytotoxic conditioning effects, infections, relapse and graft vs. host disease (GVHD). To reduce the occurrence of such complications, approaches for depleting graft T cells, partially depleting specific T cell subsets, and *ex vivo* manipulation of donor T cells have been developed (1,2). Although these methods have limited BMT-associated toxicity and GVHD, T cell depletion also negatively affects the effectiveness of adaptive immunity against viruses, fungal pathogens, and cancer cells.

Following allogenic BMT, the recovery of myeloid cells that participate in innate immunity occurs within weeks or months, whereas lymphoid cells for adaptive immunity may require up to 2 years for recovery based on quantitative and qualitative reconstitution studies of functional T cell compartments following BMT (3). T cell recovery following BMT is accomplished through two pathways. In the thymus-independent pathway, the initial recovery of T cells for regaining immune competency following allogenic BMT primarily involves the peripheral expansion of memory T cells transferred from the donor T cell pool or host cells that survive pre-BMT cytotoxic conditioning. The conditioning regimen is used to secure the available space of donor graft following BM cell depletion and reduce overall tumor mass in the recipient. Alternatively, the thymus-dependent pathway leads to the eventual reconstitution of a full repertoire of diverse, self-tolerant and naïve T cells from the host thymus via the *de novo* production of T cells (4). In the thymus-dependent recovery of T cells, crosstalk between thymic stromal cells and developing thymocytes must be regulated. However, this regulation can be restricted by damaged or altered thymic niches due to pre-conditioning regimens, infections, GVHD, or recipient age (5,6). The function of thymic epithelial cells (TECs) in T cell development is related to the development of immature thymocytes into competent T cells that respond to foreign antigens, but are self-tolerant. Essential extracellular factors for TEC development include fibroblast growth factor

(FGF)7 (7,8) and FGF10 from mesenchymal cells. Thymus growth is attenuated in mice lacking FGF-R2IIIb, a receptor for FGF7 and FGF10 (9). In addition, FGF7 administration in GVHD mice has been shown to exert a protective effect on the thymic epithelium (10), and bone morphogenic protein 4 from thymic endothelial cells contributes to endogenous regeneration following thymic damage (11). Furthermore, medullary thymic epithelial cells can transfer host antigens to CD8α dendritic cells via CD36 to induce tolerance following allogenic BMT (12). FMS-like tyrosine kinase 3 ligand (FLT3) is a receptor tyrosine kinase homologous to c-Kit and c-fms and is expressed on hematopoietic progenitor cells. The ligand of FLT3, FLT3L, is important for hematopoietic stem cell generation and survival *in vitro* (13) and for *de novo* thymus-derived T cell development (14). FLT3L administration increases the numbers of LSK cells, and early thymocyte progenitor precursors leads to thymopoiesis following BMT (15). For naïve T cells, IL-7 is essential for proliferation and maintenance in the periphery (16). For memory $CD4^+$ T cells, IL-7 and TCR stimulation is critical (17). By contrast, memory $CD8^+$ T cell maintenance mainly depends on IL-15, although TCR stimulation is dispensable (18). Thus, IL-7 and IL-15 primarily affect thymus-independent or peripheral reconstitution of T cells after BMT.

Delayed T cell recovery and restricted T cell diversity following allogenic BMT are associated with an increased risk of infection and cancer recurrence. To accelerate post-BMT, the thymus-dependent recovery of T cells, thymic reconstitution must be preceded by stimulation of the thymic niche and its output (i.e., recent thymic emigrants) by expanding memory T cells through cytokine action and through enhancing naïve T cell production by the recipient's thymus.

Previously, several immune regulatory effects of tonsil-derived mesenchymal stromal cells (T-MSCs) in BMT and inflammatory disease mouse models were reported. For example, TSG-6 released from T-MSCs attenuates acute GVHD responses in mice, represented by rapid reversal of weight loss and improved histological scoring of damaged organs (19). PD-L1 expressed by T-MSCs prevents Th17 differentiation and neutrophil-mediated inflammation (20,21), and T-MSCs also inhibit dendritic cell maturation and $CD4^+$ cell differentiation (22). As these effects of T-MSCs were observed in the context of adaptive immune responses of mature T cells, the possible effect of T-MSCs on the recovery of the thymus during allogenic BMT was thus examined.

The present study focused primarily on the ability of T-MSC co-transplantation to reconstitute the T cell repertoire in a thymus-dependent manner in mice undergoing allogenic BMT. The possible mechanism(s) of the effects T-MSCs on thymic regeneration following allogenic BMT were also investigated by comparatively analyzing the effects of MSCs from various origins, such as the BM or adipose tissue.

Materials and methods

Animals. In the present study, 8-week-old female BALB/c (n=40) and male C57BL/6 (n=14) mice (body weight, 18±2 g) were purchased from OrientBio. All animals were housed at 21-23°C with 51-54% humidity in a pathogen-free environment on a 12-h light/dark cycle and allowed free access to food and water. The experimental procedures were approved by the Animal Care and Use Committee of the College of Medicine, Ewha Womans University (Seoul, Korea; approval no. ESM18-0403).

Cells and cell culture. BM-MSCs, adipose tissue-derived MSCs (AT-MSCs) and T-MSCs were cultured in low-glucose Dulbecco's modified Eagle medium (DMEM; Welgene) in 100-mm cell culture plates. The BM-MSCs were purchased from the Severance Hospital Cell Therapy Center and the AT-MSCs were purchased from the American Type Culture Collection (ATCC). In the present study the T-MSCs were obtained previously (IRB File no. EUMC 2018-01-011-002) and maintained from the same patients as previously described (23). To prepare for cell injection, cells were collected at 80% confluence with trypsin treatment followed by 3 washes with PBS. Prior to injection with BM cells (BMCs) into the mice, MSCs were resuspended with low-glucose DMEM at a final volume of 200 μl for tail vein injection. To generate conditioned medium (CM) to analyze cellular soluble factors, cells at 80% confluence were washed four times with PBS, and the medium was replaced with serum-free DMEM. The medium was collected after 48 h of culture as previously described (19), centrifuged at 190 x g for 5 min at 25°C, passed through a 0.2-μm filter (Merck Millipore), and concentrated 20-fold by high-speed centrifugal filtration (Sorvall LYNX4000, Thermo Fisher Scientific, Inc.). The concentrated CM was then frozen and stored at -80°C for future use. As a negative control, serum-free culture medium was processed using the same method.

Allogenic BMT. Female BALB/c recipient mice were injected with busulfan (Bu; 20 mg/kg/day) for 4 days, followed by cyclophosphamide (Cy; 100 mg/kg/day) as previously described (23) for 2 days via intraperitoneal injection. After 1 day of rest, BMT was performed. To isolate BMCs, male C57BL/6 donor mice were sacrificed by cervical dislocation. Their BM was dislodged from the medullary cavities of both the femurs and tibias and prepared as a single-cell suspension. The cells were filtered using a cell strainer (70 μm, SPL Life Sciences) and centrifuged at 190 x g for 5 min at room temperature. The pellet was resuspended with ACK lysis buffer (150 mM NH_4Cl, 10 mM $KHCO_3$ and 0.1 mM Na_2EDTA) to lyse erythrocytes. Female BALB/c recipient mice were then injected with $1x10^7$ BMCs (Bu-Cy+BMT group) or $1x10^7$ BMCs combined with $2x10^6$ T-MSCs (Bu-Cy+BMT+T-MSC group) in a total volume of 200 μl via lateral tail vein injection. During the experimental periods, humane endpoints were defined as the time when the animal lost 20% of its starting weight, at which point the animal was immediately sacrificed. Recipient mice were examined daily for 40 days, and their survival and changes in weight were recorded. Mice were sacrificed by cervical dislocation on days 3, 10 and 40 following allogenic BMT. Thymus size was estimated by pixel calculations of the images using ImageJ software (version 1.51).

Immunohistochemistry. Thymus tissues were isolated from healthy recipient female BALB/c mice (normal controls), mice receiving cytotoxic conditioning (Bu-Cy only group),

Bu-Cy + BMT mice and Bu-Cy + BMT + T-MSC mice and were embedded in paraffin. Sections of the thymus were stained with hematoxylin (YD Diagnostics) for 2 min and eosin (Sigma-Aldrich) for 1.5 min (H&E) at room temperature. For immunohistochemistry, the thymus tissue sections were deparaffinized by immersion in xylene 2 times for 5 min and then hydrated. The slides were washed with PBS. The antigenic epitopes were recovered with heat using citrate buffer (10 mM citric acid and 0.05% Tween-20, pH 6.0) at 95°C for 20 min, and the slides were held in cool citrate buffer for 20 min. Endogenous peroxide blockade was performed using hydrogen peroxide (Dako North America, Inc.) in a humidity chamber for 30 min. The slides were washed again with PBS for 5 min. Non-specific binding blockade was performed with protein blocking reagent (Dako North America, Inc.) for 15 min. The slides were incubated overnight at 4°C with primary anti-CD3E rabbit polyclonal antibody (bs-4815R, Bioss Antibodies) diluted 1:200 with PBS. After returning to room temperature, the slides were washed with PBS for 5 min and incubated with secondary biotinylated anti-rabbit and anti-mouse antibodies in PBS containing carrier protein and 0.015 mol/l sodium azide (K0609, LSAB2 System-HRP, Dako North America, Inc.) in a humidity chamber for 30 min. The slides were washed with PBS for 5 min and incubated with streptavidin conjugated to horseradish peroxidase (HRP) in PBS (Dako North America, Inc.) for 30 min. The slides were washed for 5 min with PBS, and the reaction was developed with 3,3'-diaminobenzidine solution (Dako North America, Inc.) for 10 min. The slides were washed in running water for 10 min and counterstained with hematoxylin for 60 sec. The slides were washed again in running water for 5 min, dipped 3 times in 1% acid alcohol, washed in running water for 5 min, dehydrated and mounted. Immunohistochemical analysis was performed with a slide scanner (Aperio Scanscope FL).

Terminal deoxynucleotidyl transferase dUTP nick-end labeling (TUNEL) assay. The TACS®2 TdT-Fluor In Situ Apoptosis Detection kit (Trevigen, Inc.) was used to measure apoptosis in accordance with the manufacturer's protocol. Briefly, the thymus section slides were deparaffinized by warming to 57°C for 5 min, immersing twice in xylene for 5 min, and immersing consecutively in 100, 95 and 70% ethanol for 5 min each. The tissue slides were washed twice in 1X PBS for 5 min each. For labeling preparation, the slides were carefully dried around the samples, which were covered with 50 µl proteinase K solution, incubated for 15 min at room temperature, and washed twice in deionized water for 2 min each. The slides were immersed in 1X terminal deoxynucleotidyl transferase (TdT) labeling buffer for 5 min, covered with 50 µl labeling reaction mix, and incubated at 37°C for 1 h in a humidity chamber. The slides were immersed in 1X TdT stop buffer for 5 min at room temperature to stop the labeling reaction and then washed twice in deionized water at room temperature for 5 min each time. The slides were covered with 50 µl strep-fluor solution, incubated for 20 min at room temperature in the dark, and washed twice in 1X PBS for 2 min each time. After mounting (Vector Laboratories, Inc.), the samples were viewed with a confocal microscope (Carl Zeiss AG).

T cell receptor (TCR)β sequencing. Thymic RNA from experimental mice was extracted using the RNeasy Plus Mini kit (Qiagen GmbH) in accordance with the manufacturer's protocol. The RNA samples were analyzed for purity and concentration using a BioPhotometer® D30 (Eppendorf). The RNA samples were sent to Macrogen for TCRβ chain sequencing. The V-C primer was designed to cover V-D-J-C genes averaging 380 bp. The resulting sequences were analyzed using the iRepertoire TCR beta sequencing panel (https://www.irepertoire.com). To quantitatively represent the degree of T cell diversity within the samples, diversity 50 (D50) analysis was used. The D50 value is the percent of dominant and unique T cell clones that cumulatively account for 50% of the total complementarity determining region 3 (CDR3) sequences in each sample. The more diverse a library, the closer the value will be to 50. The D50 was calculated as follows: (Number of unique CDR3s that compose 50% of the reads of the top 10,000 unique CDR3s x100)/10,000=D50. An illustrative tree map was used to illustrate V-J-unique CDR3s. The entire plot area was divided into sub-areas according to V usage that were further grouped according to J usage. Each unique CDR3 within a given V-J-combination was subsequently represented by a rounded rectangle. The unevenness of squares reflects areas of thymus-dependent clonal expansion of the thymocyte repertoire.

Reverse transcription-polymerase chain reaction (RT-PCR). To compare the expression levels of FGF7, FLT3L, interleukin (IL)-7 and IL-15 in the T-MSCs compared with those from BM-MSCs and AT-MSCs, total RNA was extracted from the cells harvested at 80% confluence. Cells were collected with a cell scraper and centrifuged at 190 x g for 5 min. Cell pellets were resuspended completely with 1 ml TRIzol (Invitrogen; Thermo Fisher Scientific, Inc.) and incubated for 5 min at room temperature. The samples were added to 200 µl chloroform, inverted for 15 sec, and incubated at room temperature for 3 min. The samples were centrifuged at 16,000 x g for 15 min at 4°C. The aqueous phase was transferred into a new tube with 500 µl isopropyl alcohol and incubated at room temperature for 10 min. The samples were centrifuged at 16,000 x g for 10 min at 4°C. The supernatant was removed, and the pellet was washed with 75% ethanol. The pellet was inverted 5-6 times and centrifuged at 16,000 x g for 5 min at 4°C. The RNA pellet was dried briefly and dissolved in RNase-free water. RNA samples were analyzed for purity and concentration using a BioPhotometer® D30 (Eppendorf) and adjusted to 1 µg/µl. Total RNA was transcribed into cDNA using a reverse transcription regent (ELPIS-Biotech, Inc.) according to the manufacturer's instructions. The samples were then mixed with their respective primers and Maxime™ PCR PreMix (i-Taq, iNtRON Biotechnology) according to the manufacturer's instructions. Amplification was performed in duplicate with 35 cycles of a 30-sec denaturation step at 94°C, 30-sec annealing step at 62°C, and 30-sec extension step at 72°C. The relative fold expression and changes were observed from DNA gel electrophoresis (AE-9000 E-graph, ATTO-Gentaur). Primers for the gene expression by RT-PCR were as follows: Human *FGF7* (123 bp) forward, 5'-TCC TGC CAA CTT TGC TCT ACA-3' and reverse, 5'-CAG GGC TGG AAC AGT TCA CAT-3'; human *FLT3L* (196 bp) forward, 5'-AAA ATC CGT

GAG CTG TCT GAC-3' and reverse, 5'- TGA CAA AGT GTA TCT CCG TGT TC-3'; human *IL-7* (220 bp) forward, 5'-TTC CTC CCC TGA TCC TTG TTC-3' and reverse, 5'- CTT GCG AGC AGC ACG AAA TA-3'; human *IL-15* (190 bp) forward, 5'-TTG GGA ACC ATA GAT TTG TGC AG-3' and reverse, 5'-AGA GAA AGC ACT TCA TTG CTG TT-3'; and human *GAPDH* (192 bp) forward, 5'- GGT AAA GTG GAT ATT GTT GCC ATC AAT G-3' and reverse, 5'-GGA GGG ATC TCG CTC CTG GAA GAT GGT G-3'. The pixel densities of the *FGF7*, *FLT3L*, *IL-7* and *IL-15* bands were divided by the pixel densities of the corresponding *GAPDH* bands for normalization of the expression levels using UN-SCAN-IT-gel 6.1 software (Silk Scientific, Inc.).

Western blot analysis. Equal amounts of concentrated CM (20 μl for 2×10^5 cells) from BM-MSCs, AT-MSCs and T-MSCs were loaded onto a 5% stacking/10% separating polyacrylamide gel, separated by electrophoresis, transferred to polyvinylidene difluoride (PVDF) membranes, blocked with 5% skim milk in TBST (50 mM Tris-HCl, pH 7.6, 150 mM NaCl, 0.1% Tween-20) and incubated with primary antibodies overnight at 4˚C. All primary antibodies were prepared by diluting in 3% BSA (Bovogen Biologicals) and 0.02% sodium azide (Sigma-Aldrich; Merck KGaA) in TBST. Anti-FGF7 mouse monoclonal antibody (sc-365440, 1:200, F-9, IgG$_1$, κ), anti-FLT3L mouse monoclonal antibody (sc-365266, 1:200, F-6, IgG$_1$, κ) and anti-β-actin mouse monoclonal antibody (sc-47778, 1:3,000, C4, IgG$_1$, κ) were purchased from Santa Cruz Biotechnology, Inc. The PVDF membranes were washed 3 times for 10 min in TBST and incubated with goat anti-mouse IgG (H + L)-HRP antibody (#1706516, Bio-Rad Laboratories, Inc.) and diluted in TBST (1:3,000) for 1 h at room temperature. Following incubation, the membranes were washed 3 times for 10 min in TBST and developed using EZ-Western Lumi Femto (DoGenBio Co.). Images were obtained using ImageQuant LAS 500 (GE Healthcare Life Sciences). The pixel densities of the FGF7 and FLT3L bands were divided by the pixel densities of the corresponding β-actin bands for protein quantitation using UN-SCAN-IT-gel 6.1 software.

Statistical analysis. Data are presented as the means ± standard error of the mean (SEM). Statistical significance was determined by mixed analysis of variance (ANOVA) in conjunction with the Sidak test as applied to the weight loss of Bu-Cy pre-conditioned mice. Survival curves were plotted using Kaplan-Meier estimates and analyzed using the log-rank test. One-way ANOVA in conjunction with Sidak's multiple comparisons test were used for the results of immunohistochemistry, TUNEL assay, and semi-quantitative PCR. All analyses were performed using Prism 8 (GraphPad Software, Inc.). P<0.05 was considered to indicate a statistically significant difference for all comparisons.

Results

T-MSCs promote weight recovery and survival in allogenic BMT following Bu-Cy conditioning. To identify the effects of T-MSCs on body weight recovery and survival rate following allogenic BMT, mice were injected with Bu-Cy for cytotoxic
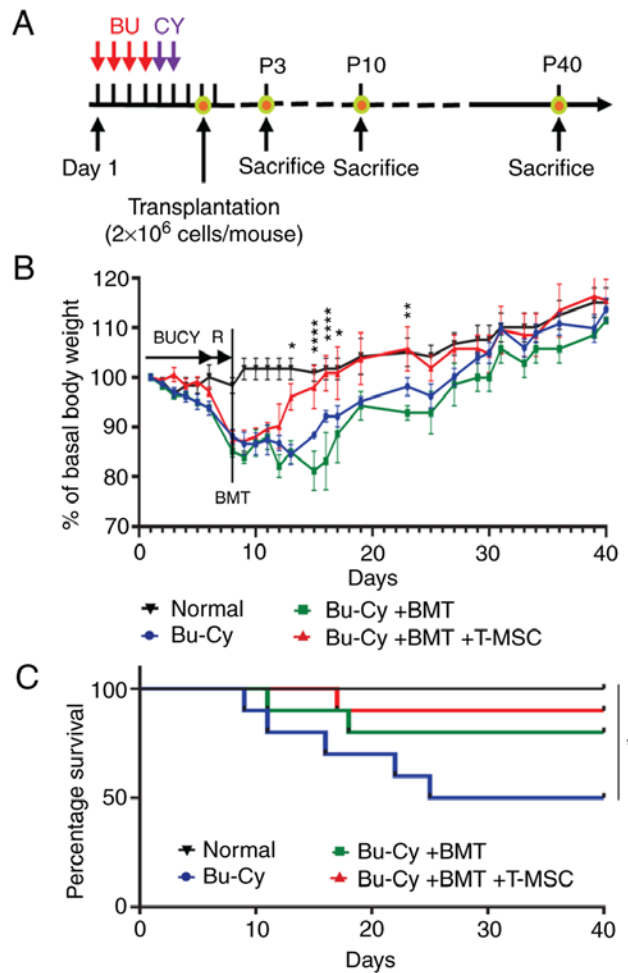

Figure 1. Weight change and survival course in the experimental mice. (A) Experimental scheme for BMT and T-MSC transfer time schedule. (B) BALB/c female mice were injected with busulfan (Bu; 20 mg/kg/day) for 4 days, followed by cyclophosphamide (Cy; 100 mg/kg/day) for 2 days. The mice were classified into 4 groups as follows: Normal female BALB/c (normal control), Bu and Cy treatment only (Bu-Cy), transplantation of BMCs from C57BL/6 mice after Bu-Cy treatment (Bu-Cy + BMT), and transplantation of BMCs plus T-MSCs after Bu-Cy treatment (Bu-Cy + BMT + T-MSC). The graph presents body weight changes in experimental mice (n=10 for each group) for 40 days after BMT. Basal body weight was determined as weight at BMT day (start). Mixed ANOVA followed by the Sidak test; *P<0.05, **P<0.01, and ****P<0.0001, Bu-Cy + BMT group vs. Bu-Cy + BMT + T-MSC group. (C) Survival course of the 4 experimental groups measured using the Kaplan-Meier estimator and compared using log-rank test (*P<0.05, P=0.0268). BMT, one marrow transplantation; T-MSC, tonsil-derived mesenchymal stromal cell; Bu-Cy, busulfan-cyclophosphamide.

conditioning and/or transplanted BMCs and BMCs with T-MSCs by tail vein injection and were observed for 40 days after cell transfer (Fig. 1A). Rapid weight loss was observed within 7 days in mice after the Bu-Cy injection, but not in the normal control (no treatment) mice (Fig. 1B). Differences in body weight recovery of the Bu-Cy + BMT + T-MSC group were noted after experimental day 14. Mice co-transplanted with T-MSCs significantly regained their body weight more rapidly than the Bu-Cy only group and Bu-Cy + BMT mice. Although body weight recovery of the Bu-Cy + BMT mice was less than that of the Bu-Cy mice, their survival rate was much higher (Fig. 1B). There are 3 different levels of intensity in the pre-conditioning regimen, such as myeloablative (high dose), reduced intensity, or non-myeloablative (24). Due to
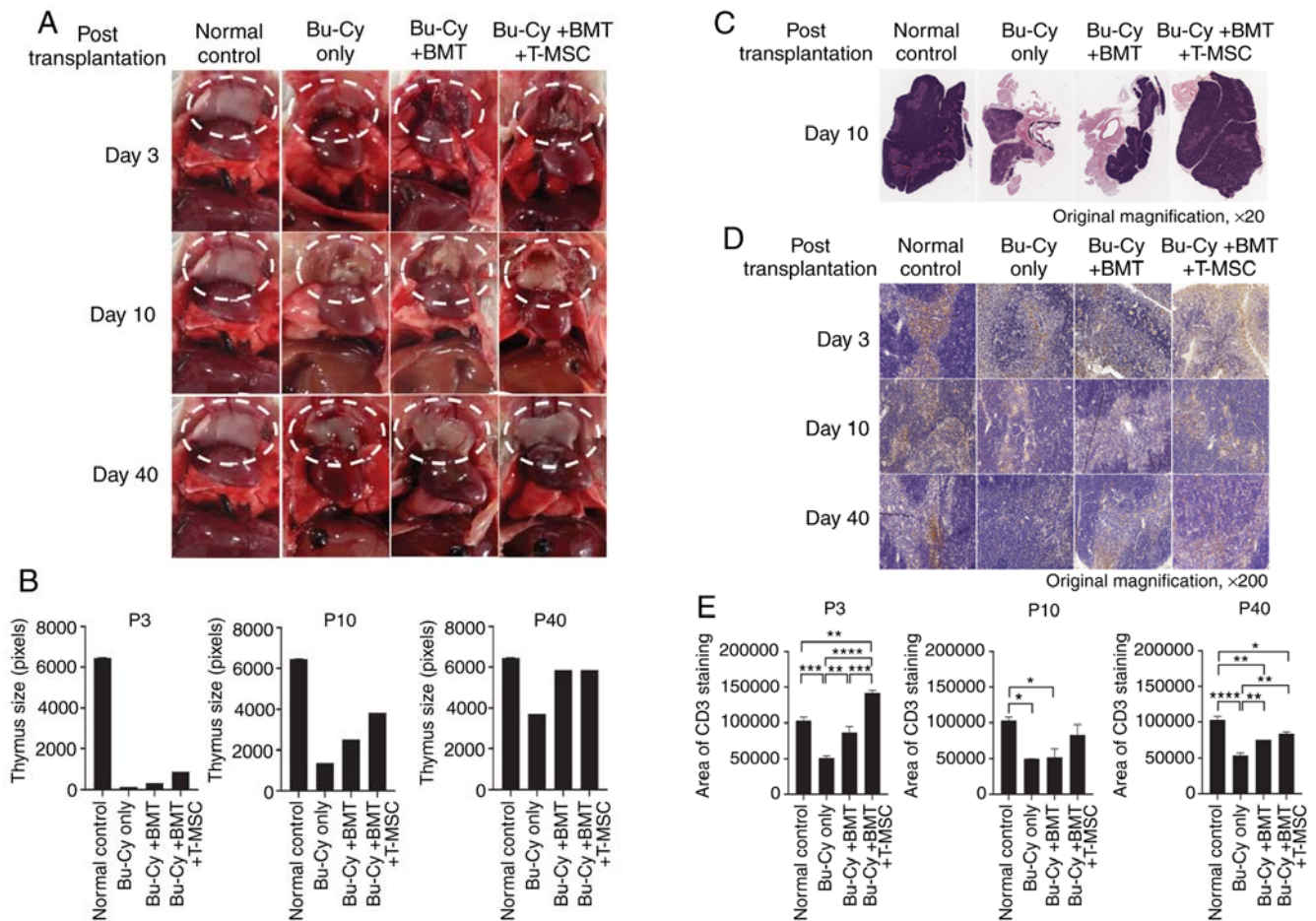
Figure 2. Thymus regeneration following BMT with T-MSC co-transplantation. (A and B) Thymus size in experimental mice at sacrifice. Shown are thymuses on days 3, 10 and 40 following allogenic BMT with or without T-MSCs. (B and C) Hematoxylin and eosin staining of thymus tissue. Original magnification, x40. (D) Histological tissue sections of thymuses collected from experimental mice on days 3, 10 and 40 post-BMT were stained with anti-CD3 antibody and hematoxylin dye (original magnification, x200). (E) Quantification of CD3$^+$ cells in thymus sections. One-way ANOVA followed by Sidak's multiple comparisons test; $^*P<0.05$, $^{**}P<0.01$, $^{***}P<0.001$ and $^{****}P<0.0001$ as indicated. BMT, one marrow transplantation; T-MSC, tonsil-derived mesenchymal stromal cell; Bu-Cy, busulfan-cyclophosphamide.

severe pre-conditioning, the Bu-Cy group exhibited high rates of fatality during the experimental period without BM cells, due to severe weight loss following cytotoxic preconditioning (2 mice died on their own from weight loss (21 and 23% weight loss for each of the mice, respectively) and 3 mice had reached the humane endpoint, which was a ≥20% loss of body weight from the starting body weight). By contrast, the Bu-Cy + BMT and Bu-Cy + BMT + T-MSC groups exhibited extended survival times; specifically, Bu-Cy + BMT and Bu-Cy + BMT + T-MSC mice exhibited an 80 and 90% survival rate, respectively, during the experimental period (Fig. 1C).

T-MSCs accelerate thymus regeneration following cytotoxic conditioning. The thymus size of the experimental mice decreased after pre-conditioning (Fig. 2A and B). To observe the effects of T-MSCs on thymus size following Bu-Cy treatment, mice from each group were sacrificed on days 3, 10 and 40 post-BMT. Gross observations revealed a shrunken thymus in the mice on day 3. On day 10, however, the thymuses of the Bu-Cy + BMT + T-MSC mice were larger than those of mice in all other groups. Thus, BMT combined with T-MSCs rapidly reversed thymus involution induced by the conditioning

regimen. On day 40, the thymus size of all groups recovered to a level similar to that of the normal control (Fig. 2B).

To analyze cellularity and recovery of thymus architecture, tissue sections were stained with H&E. Moreover, immunohistochemical analysis of thymus tissue for the T cell marker, CD3, revealed compositional changes of the thymus following BMT and indicated its restoration. The medulla and cortex regions in the thymus were distinct in the normal control groups, while thymus organization was abolished and the medulla and cortex were not distinguished in Bu-Cy only mice. The thymuses of the Bu-Cy only group exhibited less cellularity, and most of the tissue was fibrotic compared with the other groups (Fig. 2C). However, thymocyte cellularity in the Bu-Cy + BMT + T-MSC mice was more prominent than that of the other experimental groups. In addition, the thymic cortex and medulla structures of Bu-Cy + BMT + T-MSC mice were defined as clearly as those in the normal control (Fig. 2C). To further determine the recovery and repopulation of thymocytes, the thymus tissues were stained with anti-CD3 antibody and quantified areas of CD3$^+$ cells. The co-transplantation group (Bu-Cy + BMT + T-MSCs) exhibited more repopulated CD3$^+$ cells than those of the Bu-Cy only or Bu-Cy + BMT groups following BMT (Fig. 2D and E).
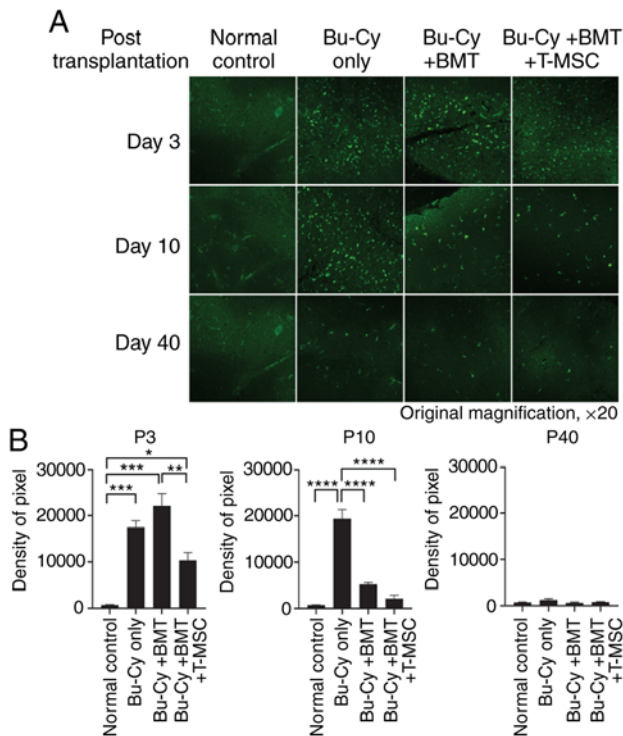
Figure 3. *In situ* detection of apoptosis in thymus tissue sections. (A) The apoptotic cells in thymus tissue from experimental mice were detected by TUNEL assay. Green fluorescence (FITC), representing apoptotic cells, was viewed by confocal microscopy. (B) The pixel densities of fluorescence were calculated using ImageJ software. Data are presented as the means ± standard error of the mean (One-way ANOVA followed by Sidak's multiple comparisons test; $^*P<0.05$, $^{**}P<0.01$, $^{***}P<0.001$ and $^{****}P<0.0001$ as indicated). BMT, one marrow transplantation; T-MSC, tonsil-derived mesenchymal stromal cell; Bu-Cy, busulfan-cyclophosphamide.

Co-transplantation of T-MSCs reduces the frequency of apoptosis. A TUNEL assay was performed to verify the effects of T-MSC co-transplantation on thymus recovery in the context of thymocyte apoptosis. Thymus sections from all experimental groups exhibited high levels of apoptosis on day 3 post-BMT. On day 10, the highest number of apoptotic cells in the thymus were observed in the Bu-Cy only group, followed by the Bu-Cy + BMT and Bu-Cy + BMT + T-MSC groups (Fig. 3A and B). All thymic sections from the experimental groups exhibited similarly low levels of fluorescence on day 40 and baseline apoptosis frequency (Fig. 3B, P40). Thus, results revealed that the co-transplantation of T-MSCs distinctly decreased the appearance of apoptotic lymphocytes in the thymus.

Co-transplantation of T-MSCs with BMCs improves diversity of the TCR repertoire. The thymic TCR repertoires of the experimental groups were compared by TCRβ chain sequencing. The squares represent areas of clonal expansion within the sample (Fig. 4A). The Bu-Cy only group exhibited the least amount of TCR repertoire diversity on day 3 post-BMT among all groups. However, at 40 days post-BMT, the Bu-Cy + BMT group exhibited the least TCR diversity.

Expression of factors related to thymus regeneration. To explore T-MSC-associated factors related to thymus regeneration, the expression of FGF7, FLT3L, IL-7 and IL-15 was measured, which are soluble factors that promote T cell reconstitution in BM-MSCs, AT-MSCs and T-MSCs using RT-PCR and western blot analysis. At the mRNA level, T-MSCs highly expressed *FGF7* and *FLT3L* compared with the BM-MSCs (P<0.05; Fig. 5A and B). At the protein level, T-MSCs highly expressed FGF7 and FLT3L compared to the BM-MSCs and AT-MSCs (Fig. 5C). Moreover, the T-MSCs produced higher levels of factors related to thymus regeneration than BM-MSCs and AT-MSCs as shown by western blot analysis (Fig. 5D). To confirm whether the factors associated thymus regeneration were increased, the expression of mouse *Fgf7*, *Flt3l*, human *FGF7* and *FLT3L* were compared in the thymuses on days 3 and 10 post-BMT. In the thymus on day 3 post-BMT, *Fgf7* and *FGF7* was significantly more expressed in the Bu-Cy + BMT + T-MSCs group than the other groups and *Flt3l* was more expressed in both BMT groups than in Bu-Cy only group (Fig. S1A and C). In the thymus on day 10 post-BMT, *Fgf7*, *Flt3l* and *FLT3L* expression levels in Bu-Cy only group were restored up to those of the normal control (Fig. S1B and D).

Discussion

In the present study, it was found that the co-transplantation of T-MSCs with BMCs accelerates the recovery of the involuted thymus after partial pre-BMT conditioning with Bu-Cy treatment. The co-transplantation of T-MSCs with BMCs replenished CD3$^+$ cell populations by inhibiting the apoptosis of thymocytes following cytotoxic pre-conditioning. In addition, T-MSC co-transplantation improved TCR repertoire expansion and increased the diversity of thymus-derived T cells.

Full T cell reconstitution following BMT needs *de novo* production of naïve T cells in the thymus of the recipient via thymus-dependent pathway. Such endogenous T cell regeneration result in increasing TCR repertoire and antigen specificity as well as long lasting immune recovery (6). Critically, the recovery of the thymus is essential for the reconstitution of immune tolerance after BMT. Patients who develop chronic GVHD exhibit reduced CD4 TCR diversity compared to those without GVHD; naïve T cell reconstitution through the thymus-dependent pathway was also observed in the non-GVHD patients (25,26). These findings suggest that peripheral T cell expansion via the thymus-independent pathway may be associated with development of GVHD. Clinically, GVHD is associated with damage to the gut, liver and skin but thymus is proven to be sensitive target of alloreactive T cells in murine model (27). Paradoxically, the most common treatment of GVHD is corticosteroids, which lead to acute thymic involution (28), eventually mediate thymic damage and lead to constriction of T cell repertoire. Therefore, a different approach is required to repress the thymus-independent pathway, but enhance thymus-dependent T cell production, as shown in the present study. In this experimental system, it was found that T-MSCs express more *FGF7* and *FLT3*L than BM-MSC or AT-MSC, but not for *IL-7* or *IL-15*, which are related to thymus-independent recovery (Fig. 5). As these results are relevant models of non-GVHD patients and focus on thymus-dependent T cell production, the effects of T-MSCs on the thymus in a GVHD model remain to be elucidated.
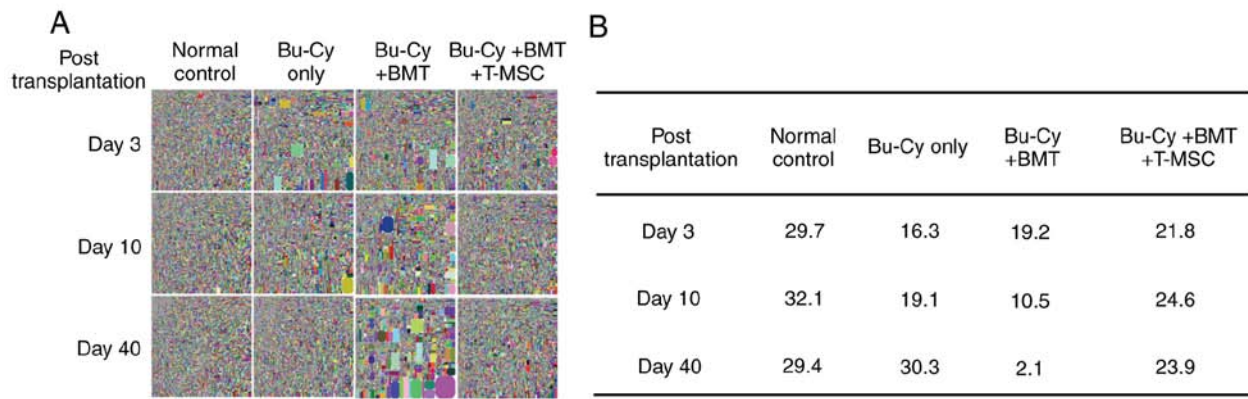
Figure 4. TCR repertoire diversity. (A) Thymus tissue samples were collected on days 3, 10 and 40 following BMT. RNA was analyzed using iRepertoire® T cell receptor β sequencing to determine T cell repertoire diversity. In the tree maps, each rounded rectangle represents a unique entry, and the area of the rectangle represents its relative frequency. (B) The D50 value represents the relative CD3-based T cell diversity of a library. BMT, one marrow transplantation; T-MSC, tonsil-derived mesenchymal stromal cell; Bu-Cy, busulfan-cyclophosphamide.
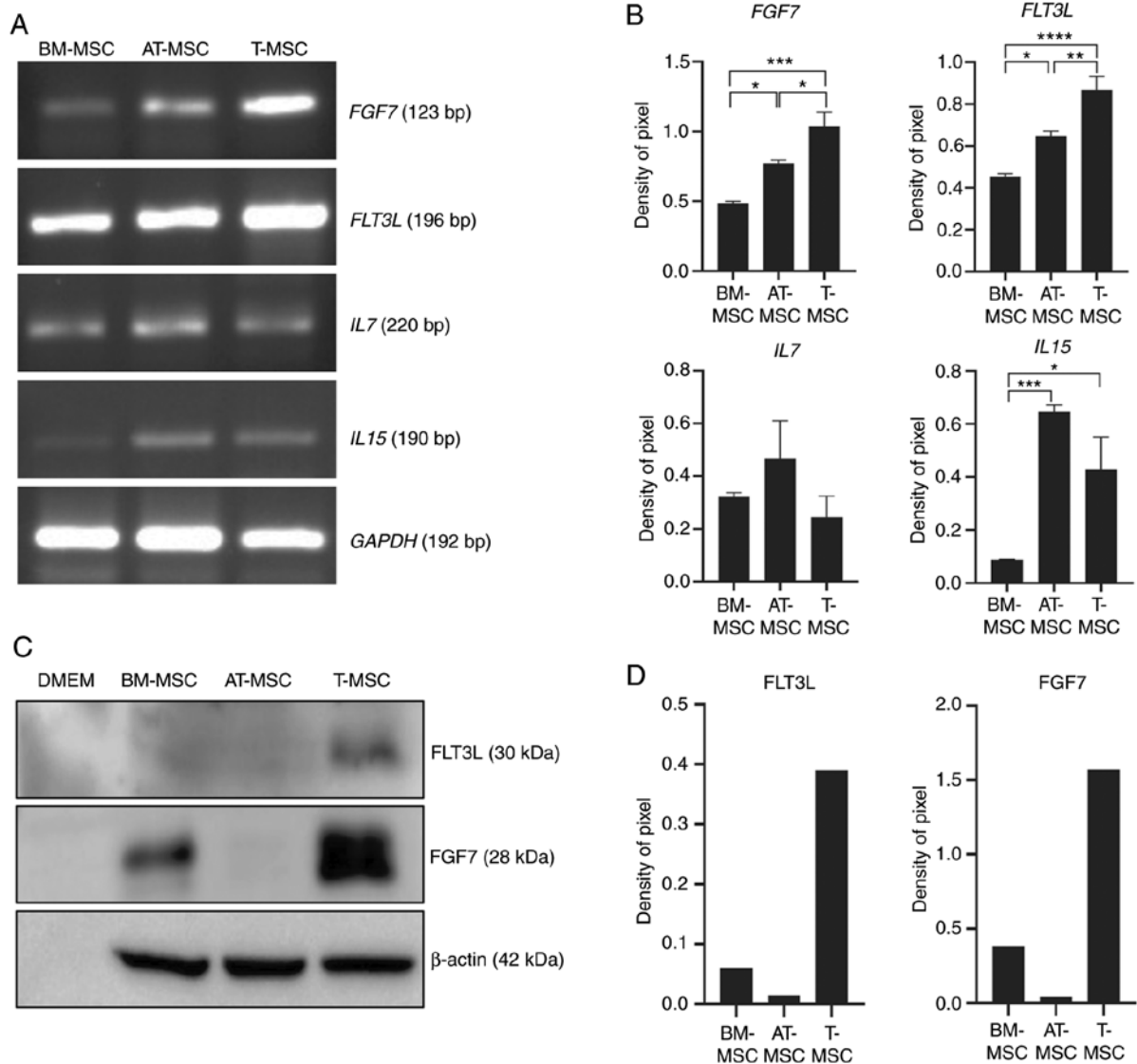

Figure 5. Expression of factors related to thymus regeneration. (A) RNA was extracted from BM-MSCs, AT-MSCs, and T-MSCs at 80% confluence and analyzed by RT-PCR. (B) The pixel densities of the *FGF7*, *FLT3L*, *IL7* and *IL15* bands were divided by the pixel densities of the corresponding *GAPDH* bands. Data are presented as the means ± standard error (one-way ANOVA followed by Sidak's multiple comparisons test; *P<0.05, **P<0.01, ***P<0.001 and ****P<0.0001 as indicated). (C) Cell culture medium was collected and concentrated for immunoblotting to detect the expression of FLT3L and FGF7 in BM-MSCs, AT-MSCs, and T-MSCs. DMEM was loaded as the negative control. (D) The pixel densities of the FLT3L and FGF7 bands from representative blots were divided by the pixel densities of the corresponding β-actin bands. BM-MSCs, bone marrow-derived mesenchymal stromal cells; T-MSCs, tonsil-derived mesenchymal stromal cells; AT-MSCs, adipose tissue-derived MSCs.

To assess thymic output and T cell reconstitution following allogenic BMT or cancer chemotherapy alone, the detection of excisional DNA circles generated from TCR chain rearrangement (29) and TCRβ gene sequencing have been used (30,31). In the present study, TCRβ chain sequencing was performed and D50 values were compared to determine repertoire reconstitution following BMT under various experimental conditions. To compare the effect of T-MSCs on thymic recovery, the BMT and BMT + T-MSC groups were primarily compared and it was found that T-MSC co-transplantation accelerated thymocyte rescue and expanded TCR repertoire following allogenic BMT. As shown in Fig. 4B, the diversity index of T cells from T-MSC co-transplanted mice was increased compared with those of the BMT only group. Notably, the recipient mice in the Bu-Cy + BMT and Bu-Cy + BMT + T-MSC groups were BALB/c female mice, and the donor BMCs originated from C57BL/6 male mice. Therefore, the thymic recovery of Bu-Cy + BMT and Bu-Cy + BMT + T-MSC mice involved two distinct cellular origins (i.e., BALB/c and C57BL/6) consisting of thymic chimerism. By contrast, the thymic recovery of the normal control and Bu-Cy only groups involved only the BALB/c recipient mouse cells. Interestingly, the D50 of the Bu-Cy only mice on day 40 post-BMT was nearly the same as that of the control mice. Although the overall survival rate of the Bu-Cy only group was 50% (n=5 out of 10), the mice that survived until the 40-day endpoint spontaneously recovered from the cytotoxic conditioning and regained thymic structure and function, represented as a decreased number of apoptotic cells on day 40 in Bu-Cy only group (Fig. 3B). However, as presented in Fig. 2E, the re-populated CD3$^+$ cells in the thymuses were the lowest in Bu-Cy only group and it might lead to a decreased survival compared to those of Bu-Cy + BMT group (Fig. 1C). Therefore, the interpretation of D50 must be accompanied with total T cell number and apoptotic cell fraction in the thymuses as an index of thymus recovery, especially representing expansion of selected TCRβ clones.

In order to evaluate immune reconstitution following BMT, γδ T cell reconstitution is associated with fewer infection following HSC transplantation (32). γδ T cells are innate-like effector cells and exert GVL without GVHD (33,34). Such γδ TCR repertoire analyses from peripheral blood are possibly as much effective as thymus sequencing for αβ TCR to evaluate T cell-mediated immune reconstitution. γδ TCR reconstitution following the co-transplantation of T-MSC also needs to be analyzed and compared in future studies.

A marked loss of body weight and depletion of fat and muscle storage occur following chemotherapy (35). The possible mechanism driving the increased body weight in the Bu-Cy + BMT + T-MSC group compared with the Bu-Cy only or Bu-Cy + BMT groups can be explained by the effect of MSCs on muscle loss due to Bu-Cy treatment. These muscle wasting was associated with the upregulation of ERK1/2 and p38 MAPKs (35). In airway inflammation model, MSCs down-regulate cyclooxygenase-2 via p38 and ERK/MAPK pathways (36). It has also been reported that human MSCs from Wharton's jelly may attenuate sarcopenia, which is loss of muscle mass and function, via activation of muscle satellite cells, reduction of apoptosis and reduced inflammation (37).

In conclusion, the approach used in the present study to explore the effects of T-MSCs on thymic regeneration following allogenic BMT revealed that the co-transplantation of T-MSCs with BMCs improved mouse survival, restored thymic structure, reduced apoptosis and expanded TCR diversity compared with the BMT-only group, possibly by inducing FLT3L and FGF7 expression in T-MSCs. Further studies are required to examine the mechanisms of T cell repertoire diversity expansion and to analyze peripheral T cell subsets following BMT. Additional analysis of the effects of co-transplantation on thymic and peripheral immune reconstitution may also contribute to the development of clinical approaches for preventing infection or GVHD following BMT.

Acknowledgements

Availability of data and materials

The datasets used and/or analyzed during the current study are available from the corresponding author on reasonable request.

Authors' contributions

DWC and KAC performed the experiments and wrote the manuscript. HJL, YHK and JWP analyzed the data and assisted in the writing of the manuscript. KJW and KHR interpreted the data and assisted in the writing of the manuscript. SYW designed the experiments and wrote the manuscript. All authors read and approved the final manuscript.

Ethics approval and consent to participate

The experimental procedures were approved by the Animal Care and Use Committee of the College of Medicine, Ewha Womans University (approval no. ESM18-0403).

Patient consent for publication

Not applicable.

Competing interests

The authors declare that they have no competing interests.

References

1. Klein OR, Buddenbaum J, Tucker N, Chen AR, Gamper CJ, Loeb D, Zambidis E, Llosa NJ, Huo JS, Robey N, *et al*: Nonmyeloablative haploidentical bone marrow transplantation with post-transplantation cyclophosphamide for pediatric and young adult patients with high-risk hematologic malignancies. Biol Blood Marrow Transplant 23: 325-332, 2017.

2. Sengsayadeth S, Savani BN, Blaise D and Mohty M: Haploidentical transplantation: Selecting optimal conditioning regimen and stem cell source. Semin Hematol 53: 111-114, 2016.
3. Storek J, Geddes M, Khan F, Huard B, Helg C, Chalandon Y, Passweg J and Roosnek E, et al: Reconstitution of the immune system after hematopoietic stem cell transplantation in humans. Semin Immunopathol 30: 425-437, 2008.
4. Krenger W, Blazar BR and Hollander GA: Thymic T-cell development in allogeneic stem cell transplantation. Blood 117: 6768-6776, 2011.
5. Simons L, Cavazzana M and Andre I: Concise Review: Boosting T-cell reconstitution following allogeneic transplantation-current concepts and future perspectives. Stem Cells Transl Med 8: 650-657, 2019.
6. Chaudhry MS, Velardi E, Malard F and van den Brink MR: Immune reconstitution after allogeneic hematopoietic stem cell transplantation: Time to T up the thymus. J Immunol 198: 40-46, 2017.
7. Rossi SW, Jeker LT, Ueno T, Kuse S, Keller MP, Zuklys S, Gudkov AV, Takahama Y, Krenger W, Blazar BR and Holländer GA: Keratinocyte growth factor (KGF) enhances postnatal T-cell development via enhancements in proliferation and function of thymic epithelial cells. Blood 109: 3803-3811, 2007.
8. Alpdogan O, Hubbard VM, Smith OM, Patel N, Lu S, Goldberg GL, Gray DH, Feinman J, Kochman AA, Eng JM, et al: Keratinocyte growth factor (KGF) is required for postnatal thymic regeneration. Blood 107: 2453-2460, 2006.
9. Sun L, Li H, Luo H and Zhao Y: Thymic epithelial cell development and its dysfunction in human diseases. Biomed Res Int 2014: 206929, 2014.
10. Jenkinson WE, Jenkinson EJ and Anderson G: Differential requirement for mesenchyme in the proliferation and maturation of thymic epithelial progenitors. J Exp Med 198: 325-332, 2003.
11. Wertheimer T, Velardi E, Tsai J, Cooper K, Xiao S, Kloss CC, Ottmüller KJ, Mokhtari Z, Brede C, deRoos P, et al: Production of BMP4 by endothelial cells is crucial for endogenous thymic regeneration. Sci Immunol 3: eaal2736, 2018.
12. Perry JSA, Russler-Germain EV, Zhou YW, Purtha W, Cooper ML, Choi J, Schroeder MA, Salazar V, Egawa T, Lee BC, et al: Transfer of cell-surface antigens by scavenger receptor CD36 promotes thymic regulatory T cell receptor repertoire development and allo-tolerance. Immunity 48: 1271, 2018.
13. Rasko JE, Metcalf D, Rossner MT, Begley CG and Nicola NA: The flt3/flk-2 ligand: Receptor distribution and action on murine haemopoietic cell survival and proliferation. Leukemia 9: 2058-2066, 1995.
14. Sitnicka E, Buza-Vidas N, Ahlenius H, Cilio CM, Gekas C, Nygren JM, Månsson R, Cheng M, Jensen CT, Svensson M, et al: Critical role of FLT3 ligand in IL-7 receptor independent T lymphopoiesis and regulation of lymphoid-primed multipotent progenitors. Blood 110: 2955-2964, 2007.
15. Williams KM, Moore AR, Lucas PJ, Wang J, Bare CV and Gress RE: FLT3 ligand regulates thymic precursor cells and hematopoietic stem cells through interactions with CXCR4 and the marrow niche. Exp Hematol 52: 40-49, 2017.
16. Tan JT, Dudl E, LeRoy E, Murray R, Sprent J, Weinberg KI and Surh CD: IL-7 is critical for homeostatic proliferation and survival of naive T cells. Proc Natl Acad Sci USA 98: 8732-8737, 2001.
17. Kondrack RM, Harbertson J, Tan JT, McBreen ME, Surh CD and Bradley LM: Interleukin 7 regulates the survival and generation of memory CD4 cells. J Exp Med 198: 1797-1806, 2003.
18. Murali-Krishna K, Lau LL, Sambhara S, Lemonnier F, Altman J and Ahmed R: Persistence of memory CD8 T cells in MHC class I-deficient mice. Science 286: 1377-1381, 1999.
19. Cho KA, Kim YH, Park M, Kim HJ, Woo SY, Park JW and Ryu KH: Conditioned medium from human palatine tonsil mesenchymal stem cells attenuates acute graft-vs.-host disease in mice. Mol Med Rep 19: 609-616, 2019.
20. Kim JY, Park M, Kim YH, Ryu KH, Lee KH, Cho KA and Woo SY: Tonsil-derived mesenchymal stem cells (T-MSCs) prevent Th17-mediated autoimmune response via regulation of the programmed death-1/programmed death ligand-1 (PD-1/PD-L1) pathway. J Tissue Eng Regen Med 12: e1022-e1033, 2018.
21. Cho KA, Park M, Kim YH, Ryu KH and Woo SY: Poly I:C primes the suppressive function of human palatine tonsil-derived MSCs against Th17 differentiation by increasing PD-L1 expression. Immunobiology 222: 394-398, 2017.
22. Park M, Kim YH, Ryu JH, Woo SY and Ryu KH: Immune suppressive effects of tonsil-derived mesenchymal stem cells on mouse bone-marrow-derived dendritic cells. Stem Cells Int 2015: 106540, 2015.
23. Kim YH, Cho KA, Lee HJ, Park M, Shin SJ, Park JW, Woo SY and Ryu KH: Conditioned medium from human tonsil-derived mesenchymal stem cells enhances bone marrow engraftment via endothelial cell restoration by pleiotrophin. Cells 9: 221, 2020.
24. Gyurkocza B and Sandmaier BM: Conditioning regimens for hematopoietic cell transplantation: One size does not fit all. Blood 124: 344-353, 2014.
25. Soares MV, Azevedo RI, Ferreira IA, Bucar S, Ribeiro AC, Vieira A, Pereira PNG, Ribeiro RM, Ligeiro D, Alho AC, et al: Naive and stem cell memory T cell subset recovery reveals opposing reconstitution patterns in CD4 and CD8 T cells in chronic graft vs. host disease. Front Immunol 10: 334, 2019.
26. Alachkar H and Nakamura Y: Deep-sequencing of the T-cell receptor repertoire in patients with haplo-cord and matched-donor transplants. Chimerism 6: 47-49, 2015.
27. Krenger W, Rossi S and Hollander GA: Apoptosis of thymocytes during acute graft-versus-host disease is independent of glucocorticoids. Transplantation 69: 2190-2193, 2000.
28. Ashwell JD, Lu FW and Vacchio MS: Glucocorticoids in T cell development and function. Annu Rev Immunol 18: 309-345, 2000.
29. Douek DC, Vescio RA, Betts MR, Brenchley JM, Hill BJ, Zhang L, Berenson JR, Collins RH and Koup RA: Assessment of thymic output in adults after haematopoietic stem-cell transplantation and prediction of T-cell reconstitution. Lancet 355: 1875-1881, 2000.
30. Seo YD, Jiang X, Sullivan KM, Jalikis FG, Smythe KS, Abbasi A, Vignali M, Park JO, Daniel SK, Pollack SM, et al: Mobilization of CD8+ T Cells via CXCR4 blockade facilitates PD-1 checkpoint therapy in human pancreatic cancer. Clin Cancer Res 25: 3934-3945, 2019.
31. Toivonen R, Arstila TP and Hanninen A: Islet-associated T-cell receptor-β CDR sequence repertoire in prediabetic NOD mice reveals antigen-driven T-cell expansion and shared usage of VβJβ TCR chains. Mol Immunol 64: 127-135, 2015.
32. Perko R, Kang G, Sunkara A, Leung W, Thomas PG and Dallas MH: Gamma delta T cell reconstitution is associated with fewer infections and improved event-free survival after hematopoietic stem cell transplantation for pediatric leukemia. Biol Blood Marrow Transplant 21: 130-136, 2015.
33. Handgretinger R and Schilbach K: The potential role of gammadelta T cells after allogeneic HCT for leukemia. Blood 131: 1063-1072, 2018.
34. Minculescu L, Marquart HV, Ryder LP, Andersen NS, Schjoedt I, Friis LS, Kornblit BT, Petersen SL, Haastrup E, Fischer-Nielsen A, et al: Improved overall survival, relapse-free-survival, and less Graft-vs.-host-disease in patients with high immune reconstitution of TCR gamma delta cells 2 months after allogeneic stem Cell Transplantation. Front Immunol 10: 1997, 2019.
35. Barreto R, Waning DL, Gao H, Liu Y, Zimmers TA and Bonetto A: Chemotherapy-related cachexia is associated with mitochondrial depletion and the activation of ERK1/2 and p38 MAPKs. Oncotarget 7: 43442-43460, 2016.
36. Gu W, Song L, Li XM, Wang D, Guo XJ and Xu WG: Mesenchymal stem cells alleviate airway inflammation and emphysema in COPD through down-regulation of cyclooxygenase-2 via p38 and ERK MAPK pathways. Sci Rep 5: 8733, 2015.
37. Wang QQ, Jing XM, Bi YZ, Cao XF, Wang YZ, Li YX, Qiao BJ, Chen Y, Hao YL and Hu J: Human Umbilical Cord Wharton's Jelly Derived mesenchymal stromal cells may attenuate sarcopenia in aged mice induced by hindlimb suspension. Med Sci Monit 24: 9272-9281, 2018.